Research Article

Journal of RAMAN SPECTROSCOPY

Received: 3 February 2009 Accepted: 8 July 2009 Published online in Wiley Interscience: 1 September 2009

(www.interscience.wiley.com) DOI 10.1002/jrs.2429

Electromagnetic field enhancement in TERS configurations

Zhilin Yang,[a,b] Javier Aizpurua[c]* and Hongxing Xu[a,d]*

We use three-dimensional finite-difference time domain (3D-FDTD) simulations to investigate the field enhancement properties of tip-enhanced Raman scattering (TERS) in order to find optimal geometric parameters of the metal tip and the metal substrate under certain excitation wavelengths with side illumination. The simulation results show that plasmon coupling effects between the metal tip and the metal substrate play the key role in TERS enhancement, and the enhancement drops dramatically as the distance between the tip and the substrate increases. The spatial resolution of TERS is mainly dependent on the radius of curvature of the tip end. A sharp tip with a small radius can dramatically increase the spatial resolution of TERS. Increasing the tip–substrate distance or changing the metallic substrate into a dielectric substrate lowers the spatial resolution. The TERS enhancement dependence on the incident angle and polarization, the size of tip, as well as the composition of the substrate is also discussed in detail.

Keywords: tip-enhanced Raman spectroscopy (TERS); finite difference time domain (FDTD); electromagnetic field enhancement

Introduction

Tip-enhanced Raman spectroscopy (TERS), which combines surface-enhanced Raman scattering (SERS) with scanning probe microscopy (SPM), such as scanning tunneling microscopy (STM), atomic force microscopy (AFM), or scanning near field optical microscopy (SNOM), provides not only rich spectral and structural information of tiny amounts of the probe molecules even down to a single-molecule level near the metal tip but also a high spatial resolution of the sample simultaneously.[1–5] The requirement that metal surfaces are roughened or nano-structured is one of the most severe restrictions in the application of SERS to a wide variety of problems. As a new technique, TERS has recently been developed to circumvent, in principle, this severe restriction and to access a more general and complete set of substrates in SERS.[6,7] The excitation of the localized surface plasmons in the tip–substrate cavity produces a large local optical electromagnetic (EM) field enhancement, as high as 2 orders of magnitude with respect to the amplitude of the incoming light, resulting in a considerable increase of the Raman intensity, the Raman signal being proportional to the fourth power of the field enhancement.[8] In addition to the large increase of the Raman intensity, the enhanced localized EM field in TERS is spatially limited to a few tens of nanometers. This localization mainly depends on the radius of curvature of the SPM tip and the tip–substrate distance. The nanometer-scale spatial resolution of TERS has been used to provide high-resolution images of nanoscale samples.[9]

It is of great importance to choose optimal conditions for achieving maximal electric near-field enhancement for a specific TERS system. Some theoretical and experimental studies have been developed to investigate the field enhancement and spatial resolution for various tip–substrate systems.[10–14] However, many variables governing the field enhancement factor and the spatial resolution in the vicinity of the tip–substrate system require a systematic understanding of the effect of the tip and substrate material, the tip size and shape, the tip–substrate distance, and the configuration of the incoming light including polarization and incidence angle. The electrodynamic calculation of the field enhancement and distribution in these cases are therefore crucial to understand the optimal performance in TERS.

To perform electrodynamic calculations of light scattering from particles of an arbitrary shape, various theoretical methods, including the finite-element method (FEM),[15,16] the discrete dipole approximation (DDA),[17,18] the finite-difference in time-domain (FDTD) method,[19–22] or the boundary element method (BEM),[23,24] and others have been used to get the field enhancement and distribution in SERS and TERS configurations. Among them, FDTD is a powerful tool to simulate the distribution of the EM field around the illuminated nanoparticle array or substrates with nonspherical geometry. In this work, the three-dimensional finite-difference time-domain (3D-FDTD) method is used to perform theoretical simulations of the field enhancement and spatial resolution of a conical gold tip, with and without a substrate, under the side illumination mode. The dependence of the tip size and shape, the substrate material, the tip–substrate distance, and the

* *Correspondence to: Javier Aizpurua, Center for Materials Physics (CFM) of the Spanish Council for Scientific Research (CSIC) and Donostia International Physics Center (DIPC), Paseo Manuel Lardizabal, Donostia-San Sebastián 20018, Spain. E-mail: aizpurua@ehu.es*

Hongxing Xu, Beijing National Laboratory for Condensed Matter Physics and Institute of Physics, Chinese Academy of Sciences, Box 603-146, 100190, Beijing, China. E-mail: hxxu@aphy.iphy.ac.cn

a *Beijing National Laboratory for Condensed Matter Physics and Institute of Physics, Chinese Academy of Sciences, 100190, Beijing, China*

b *Department of Physics, Xiamen University, 361005, Xiamen, China*

c *Center for Materials Physics (CFM) of the Spanish Council for Scientific Research (CSIC) and Donostia International Physics Center (DIPC), Donostia-San Sebastián 20018, Spain*

d *Division of Solid State Physics, The Nanometer Consortium, Lund University, S-22100, Lund, Sweden*

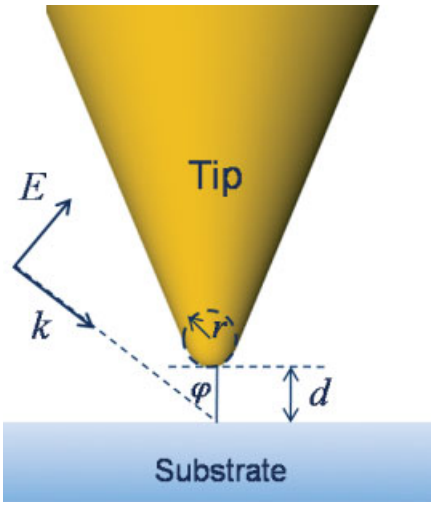

Figure 1. Schematic diagram of the metal tip and substrate geometry: the tip is modeled as a conical taper terminated by a hemisphere of radius *r*, held at a distance *d* from the substrate surface. An electromagnetic plane wave is incident at an angle φ, with the polarization in the plane of incidence.

incidence angle and polarization of the excitation light on TERS are discussed in detail.

Theoretical Model and The FDTD Method

The geometry considered for TERS in this work consists of a gold metal cone, ending in a sphere with a radius of curvature *r* in air over a substrate with tip–surface separation *d*, as depicted in Fig. 1. A p-polarized plane wave is incident from the side at an angle φ on the cavity formed by the tip and substrate. The wavelength of the incident light is set to be 632.8 nm in all simulations since the He–Ne laser is the most used excitation light source in TERS experimental studies and it usually shows an efficient TERS enhancement factor when the distance of the tip to the substrate is in the range of 1–5 nm for gold tips.

The basic principle of FDTD is to numerically solve Maxwell's differential equations.[25,26] In the FDTD approach, both space and time are divided into discrete segments. Space is segmented into box-shaped cells, and the electric fields are located on the edges of the box and the magnetic fields are positioned on the faces. This orientation of the fields is known as the Yee cell. A standard Cartesian Yee cell used for FDTD calculation is often set as a cubic voxel, and the three-dimensional space lattice is comprised of a multiplicity of such Yee cells. In order to obtain an accurate field distribution for the 3D object, the Yee cell size, which is the most important constraint in any FDTD simulation, must be much less than the smallest excitation wavelength. A convergence rule often quoted in this technique is 'ten cells per wavelength,' meaning that the side of each cell should be $\frac{1}{10}\lambda$ or a smaller fraction of the shortest wavelength of interest. Another consideration regarding the size of the cell is that the relevant geometrical features of the problem must be accurately modeled. In order to accurately simulate the 1–2 nm tip–substrate distance in a general gap mode TERS configuration, the appropriate Yee cell size should be in the range of 0.5 to 1 nm. This size will automatically meet the condition of 'ten cells per wavelength' in the simulation. However, this cell distribution would require very large memory resources and computation time when applied to simulate a real TERS geometry. In this work, the nonuniform FDTD mesh method was adopted to improve the accuracy of modeling, which reduced the computation resources needed significantly.

Benefiting from the method developed by Leubbers, Hunsberger, and Kunz, since the early 1990s it has been possible to use the FDTD method for dispersive materials based on the simple Drude model.[26–28] However, the Drude model cannot accurately describe the frequency-dependent complex permittivity for metals over a wide frequency range. Here, instead of the simple Drude model, we adopted the general Drude model to simulate the complex permittivity of the form[19,29]

$$\varepsilon(\omega) = \varepsilon_\infty + \frac{\varepsilon_s - \varepsilon_\infty}{1 + i\omega\tau} + \frac{\sigma}{i\omega\varepsilon_0} \quad (1)$$

where ε_s, ε_∞, σ, τ represent static permittivity, infinite frequency permittivity, conductivity, and the relaxation time, respectively; ω is the angular frequency; and ε_0 is the permittivity of free space. The four parameters ε_s, ε_∞, σ, τ can be adjusted through curve-fitting techniques to correctly match the complex permittivity, which can be derived from the experimentally determined optical constants through the relationship $\varepsilon_r = n^2 - k^2$, $\varepsilon_i = 2nk$, where ε_r, ε_i are the real and imaginary part of dielectric function of the dispersive material, respectively.

It is important to keep in mind that for materials that can be described through the general Drude model, the infinite frequency permittivity must meet the condition $\varepsilon_\infty \geq 1$ and the conductivity should obey the equation $\sigma \geq \frac{\varepsilon_0(\varepsilon_\infty - \varepsilon_s)}{\tau_0} 1$ if $\varepsilon_s < \varepsilon_\infty$.

This model for the local dielectric function of metallic materials represents faithfully the optical response in a wide frequency region, especially at visible frequencies, ensuring the accuracy of the FDTD simulation.[19,29]

Near-Field Coupling Effect In TERS

It is well known that an EM configuration based on a single particle is not enough in most cases to achieve efficient SERS-active systems. Most SERS-active systems are actually assemblies of coupled nanoparticles, such as nanoparticle aggregates, rough metal surfaces, and island films.[30] For example, single-molecule SERS (SM-SERS) has been limited mostly to colloidal aggregate structures, which presumably are efficient at producing particle junction structures that are needed to produce the extraordinarily high enhancement factors (EM hot spots) required for SERS.[8,31,32] Similarly, the strong near-field coupling effect between the tip and substrate usually plays a key role in producing efficient enhancement in a real TERS system. Figure 2(a) and (b) show the calculated optical field enhancement in TERS with and without a gold substrate, respectively. The Au tips are modeled as a metal cone with a radius of curvature 25 nm in both Fig. 2(a) and (b). The 632.8 nm monochromatic plane wave is incident at an angle $\varphi = 60^\circ$, with the polarization in the plane of incidence, from the side. The distance d between the tip and substrate is set to be 2 nm. In the simulation, the Yee cell size in the gap region was set to be $0.5 \times 0.5 \times 0.5$ nm^3 while a $2 \times 2 \times 2$ nm^3 cell size was used in other regions. This nonuniform FDTD mesh method can save computation resources greatly without losing accuracy. Figure 2 shows that the maximum field enhancement, defined as the ratio between the maximum local field E_{loc} and the incoming field E_{in} amplitude, $M = \frac{|E_{loc}|}{|E_{in}|}$, in a single tip is only about 20 (Fig. 2(a)), which is much smaller than the field enhancement factor of 189

Journal of RAMAN SPECTROSCOPY

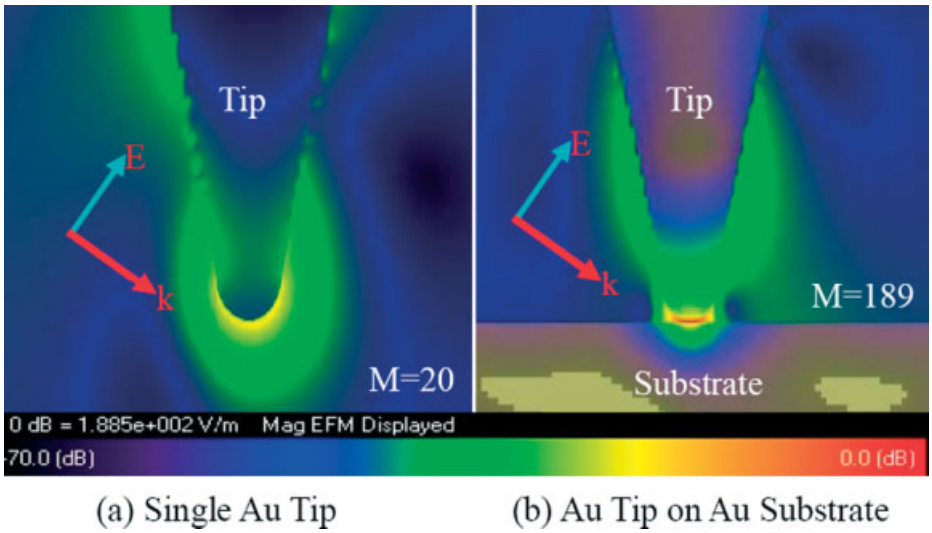

Figure 2. FDTD simulations of the electric field distribution for a single Au tip (a), and a gold tip held at distance $d = 2$ nm from a gold substrate surface. The polarization E and wave vector k of the incoming light are displayed in the schematics. *M* stands for the maximum.

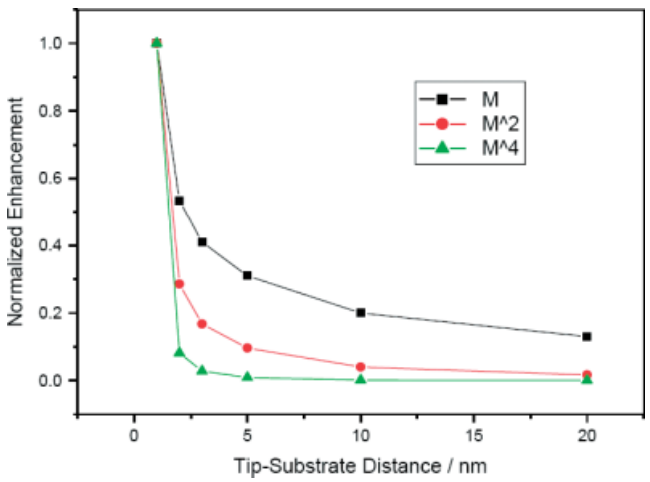

Figure 3. Dependence of field enhancement *M* (square), intensity enhancement M^2 (circle), and TERS enhancement M^4 (triangle) on the tip–substrate distance. All calculation parameters are the same as in Fig. 2(b) with a varying tip–substrate distance.

in a tip–substrate coupled system (Fig. 2(b)). Since the enhanced Raman scattering intensity from a probe molecule at any given position is approximately proportional to the fourth power of the electric field enhancement at the position of the molecule, the maximum Raman EM enhancement factor for a single gold tip is therefore about 1.6×10^5. If the tip is placed over a gold substrate with a small distance, as in Fig. 2(b), with $d = 2$ nm, the strong near-field coupling effect between the tip and substrate will result in a 1.8×10^9 TERS enhancement factor, which means four extra orders of Raman enhancement contributing to the TERS signal compared with the TERS enhancement in a single gold tip. The coupling effect in TERS is strongly dependent on the tip–substrate separation since the near field decays in an exponential manner far from the surface. Figure 3 shows the normalized decay curve of the localized field enhancement $M = \frac{|E_{loc}|}{|E_{in}|}$, the intensity enhancement M^2, and the TERS enhancement M^4, respectively. The maximum enhancement in the gap is strongly dependent on the tip–substrate distance *d*. If *d* is changed from 1 to 5 nm, the maximum electric field enhancement in the gap would decay by about 70%, and the TERS signals from the probe molecule in the gap would decay by 99%, assuming a fourth power law to describe the Raman intensity, where the energy shift of the vibration can be neglected. If the tip is placed over the substrate at a distance of 20 nm, the coupling effect is negligible according to our FDTD calculation, and the TERS enhancement becomes approximately equal to the one produced in the proximity of a single tip. It should be noted that the above coupling effect is calculated at a fixed frequency to resemble the experimental conditions. If the frequency of the excitation laser is changed, the decay curve may show some different characteristic since the plasmon resonance frequency is strongly affected by the tip–substrate distance, especially when this distance is in the range of 0–3 nm.

Tip-Size Dependence On TERS Enhancement and Spatial Resolutions

The dominant contribution producing the giant enhancement factor in TERS is associated with the large local field enhancement due to the excitation of localized surface plasmons at the tip–substrate system when illuminated by the incoming radiation. The strength of the localized surface plasmon resonance and the corresponding TERS enhancement is dependent on many factors, such as the size and shape of the tip, the materials of the tip and substrate, the distance between the tip and substrate, and the dielectric environments of TERS. In this section, we focus our attention on the tip size dependence of the TERS enhancement and the corresponding spatial resolution that can be achieved. In Fig. 4 we can observe the FDTD simulation of the maximum field enhancement at the surface of a Au substrate when probed with gold tips of different sizes under p-polarized laser excitation with a wavelength of 632.8 nm illuminated from the side at an incident angle of 60°. The tip–substrate distance is fixed in all cases at a value of $d = 2$ nm. The radius of curvature of the tip in the simulation model is in the range of 5 to 80 nm. The calculations show that the field enhancement does not change very much as the tip size changes. The value of the enhancement

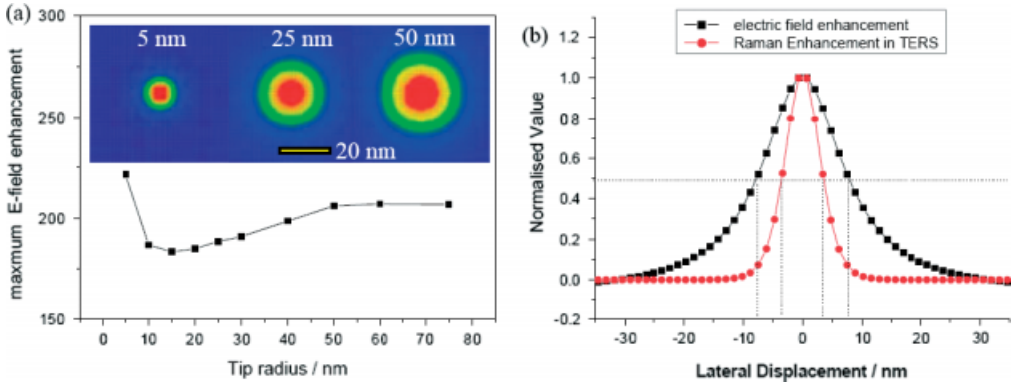

Figure 4. Tip size dependence of the maximum field enhancement and spatial resolutions of TERS. All calculation parameters, except for the tip size, are the same as in Fig. 2(b). (a) Maximum electric field enhancement in the gap as a function of tip radius. The inserts give the spatial field distribution for tip radius $r = 2$, 25, and 50 nm respectively, from left to right. The yellow scale bar is 20 nm (b): Normalized electric field enhancement M (black) and normalized Raman enhancement M^4 along a horizontal line 1 nm below the apex of a gold tip with 25 nm radius on top of a gold substrate.

factor is in the range of 180 to 220. The TERS enhancement increases slowly when the tip radius increases from 15 to 50 nm. Further increase of the tip radius does not provide additional enhancement. This increasing tendency is similar to the findings of a previous SERS study,[33] which has confirmed that gold nanoparticles with sizes of 100–130 nm give rise to the largest SERS enhancement factor under 632.8 nm laser excitation mainly due to the size-dependent effect of surface plasmon resonance. An interesting result derived from our simulation is that when the tip radius decreases from 15 to 5 nm, the enhancement in the substrate shows a rapid increasing rate, this enhancement being due to a lightning rod effect which results from the increasing confinement of the surface charge density at the sharp tip apex. We note that the lightning rod effect is a nonresonant effect that depends mainly on the radius of curvature of the TERS tip.

We consider now the spatial resolution of TERS for the different tip radii. Due to the highly localized EM fields, TERS can provide very high spatial resolution, smaller than the size of the tip apex, mainly determined by the tip geometry. The field distribution in a plane parallel to and 1 nm above the substrate is shown as an inset in Fig. 4(a) corresponding to a tip radius r of 5, 25, and 50 nm, respectively. The figure clearly indicates that the center of the area underneath the tip apex gives the highest enhancement, and the spatial resolution, which we quantify as the full width at half-maximum (FWHM) of the Raman enhancement, is strongly dependent on the tip radius. From our simulations, we can state that decreasing the tip radius can improve dramatically the spatial Raman resolutions of TERS, and therefore tips with sharp ends (small radius of curvature) are preferable in TERS. We show in Fig. 4(b) the result of an FDTD calculation for a 25-nm-radius gold tip placed on top of a gold substrate at 2-nm separation distance. The spatial resolution obtained for the TERS signal is less than 10 nm, which is better than the field resolution and intensity resolution, because of the fourth power rule in TERS enhancement. It should be pointed out here that the radius of the tip is not the only factor determining the value of the FWHM. In fact, the substrate material and the tip–substrate separation will also directly affect the spatial resolution of TERS.[10] In general, increasing the tip–substrate distance or changing the metallic substrate into a dielectric substrate will lower the spatial resolution.

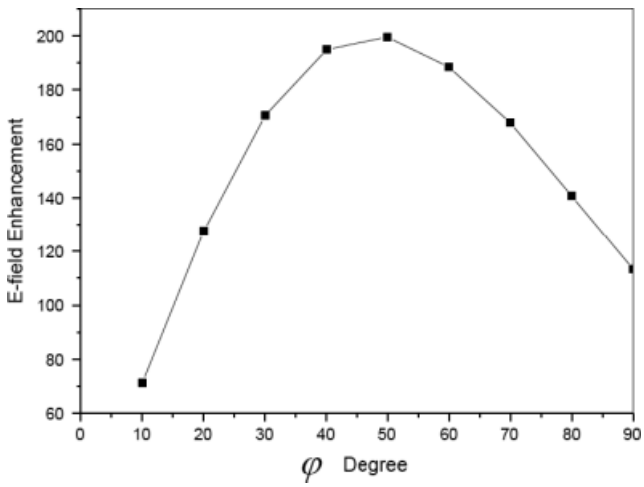

Figure 5. Dependence of field enhancement on the plane wave incident angle φ. All the calculation parameters are as in Fig. 2 (b).

Incidence Angle Dependence Of TERS Enhancement

The side-illumination geometry is the most convenient choice for analysis of nontransparent samples and samples on nontransparent substrates with TERS. In addition, side-illumination geometry provides an easier way to align the incident beam polarization along the tip axis, compared to the bottom-illumination geometry, which will be useful to optimize the TERS configuration in order to get the maximum enhancement factor. Predictions by theoretical simulations can provide important insights to choose an optimal angle of incidence giving the maximum enhancement factor for a given TERS geometry. However, there are no detailed experimental studies of the enhancement factor as a function of incidence angle to date. Since the vertical field component along the tip axis plays a dominant role in the coupling effect, it is logical to expect that the maximum field enhancement occurs when φ tends to $\frac{\pi}{2}$, as this angle maximizes the vertical field component. However, this is not the result from our simulations. Figure 5 shows the dependence of field enhancement on the incidence angle of the incoming light. The maximum field enhancement for a gold tip kept at a 2-nm distance over a gold substrate under p-polarized

Journal of RAMAN SPECTROSCOPY

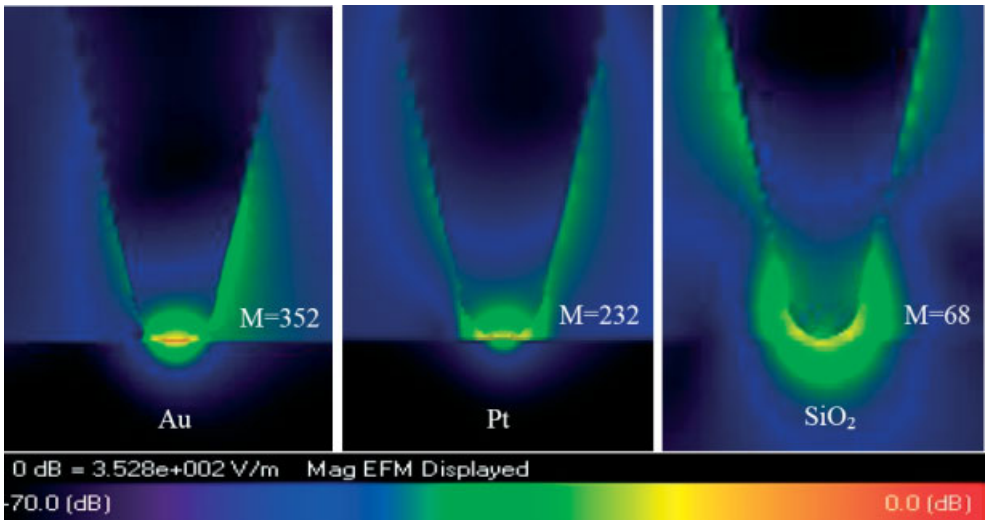

Figure 6. FDTD simulations of the electric field distribution in the proximity of a single Au tip at a distance $d = 1$ nm from an Au (left), Pt (middle), and SiO_2 (right) substrate. *M* is the maximum field enhancement.

laser illumination of wavelength 632.8 nm from the side occurs at an incidence angle φ in the range of 40–60°.

The reason for this optimal value (diagonal incidence) is due to the proximity of the surface. The total vertical field in the gap is strongly affected by the interference of the reflected field and the incident field. When $\varphi \rightarrow 90°$, although the amplitude of the reflected vertical field reaches its maximum, its phase is opposed to that of the incident field, and the interference results in a decreased intensity at the substrate surface. This result is very similar to those of previous theoretical studies.[34] However, if the p-polarized laser illumination is changed to s-polarized illumination, our simulation shows that a very small enhancement in the gap is produced, independently of the incidence angle. This is easy to understand since the incident light cannot meet the phase-matching condition for excitation of the surface plasmon polaritons at plane substrate surface.

Substrate Dependence Of TERS

It is well known that the material of the irradiated tip is another aspect of great importance to provide effective TERS enhancement. Gold and silver are the two metals commonly used for TERS tips because of their ability to create a large enhanced EM field at the tip apex due to the excitation of the localized surface plasmon polariton in visible frequencies. Experimental results and theoretical simulations have demonstrated that metallic and dielectric substrates show very different coupling strengths and therefore enhancement capabilities, for example, in infrared microscopy based on the scattering of a tip–substrate system.[35] Here, we investigate the influence of the substrate material on TERS enhancement in the cases of a noble metal (Au), a transition metal (Pt), and a dielectric material (SiO_2) acting as the substrates in our simulation. In all calculations, the gold tip is held at distance $d = 1$ nm from the substrate surface, and the p-polarized 632.8 nm plane wave is incident at the tip–substrate gap at an angle of 60°. The results in Fig. 6 show a direct effect of the substrate material on the degree of TERS enhancement. A Au substrate gives the highest field enhancement factor of 353 since it behaves as a good metal producing a large EM coupling with the tip. A Pt substrate gives an enhancement of 232. The dielectric substrate SiO_2 gives the smallest enhancement factor of 68. This result is similar to SERS properties in hosts made of different materials, and depends on the degree of coupling that the substrate can provide to the tip. Metallic gaps can provide strong surface plasmon resonances in the visible, whereas dielectric materials cannot couple so effectively, producing the effect of an isolated tip.

Field Enhancement in Double-Tip TERS

Recently, a method for achieving a larger Raman enhancement by using a double-tip TERS configuration has been reported.[13] In this novel TERS configuration, one of the pieces is a scanning gold tip and the other one is a gold nanoparticle absorbed on a flat gold surface acting as a fixed tip. The resulting Raman enhancement is several times higher than that of normal TERS. Zhang *et al*.[14] studied the influence of nanosteps on the enhancement in gap mode TERS and found that nanoscale roughness on the metal surface can increase the TERS enhancement by an order of magnitude. In order to quantitatively evaluate the EM field enhancement in a double-TERS system, we have performed a full 3D-FDTD calculation for such a system. In the simulation, we modeled the fixed tip as a 50-nm diameter gold nanoparticle, with the second tip, substrate, and excitation parameters being the same as in Fig. 2(b). The distance between the tip and the nanoparticle is 2 nm. The result of the simulation (Fig. 7) shows that the field enhancement at the tip–particle gap in double-tip TERS is about 251, in comparison with 189 of a normal single tip–substrate TERS configuration. This mechanism provides a further 30% electric field enhancement. This 251 times field enhancement results in a 4×10^9 TERS enhancement, which is in good agreement with the experimental data reported in Ref. [13].

The additional field enhancement in a double-tip TERS is mainly due to the lightning rod effect provided by the gold nanoparticle, since a larger surface charge density is produced at the sharp curvature of the small gold particle, bringing more intense coupling effect in the double-tip TERS.

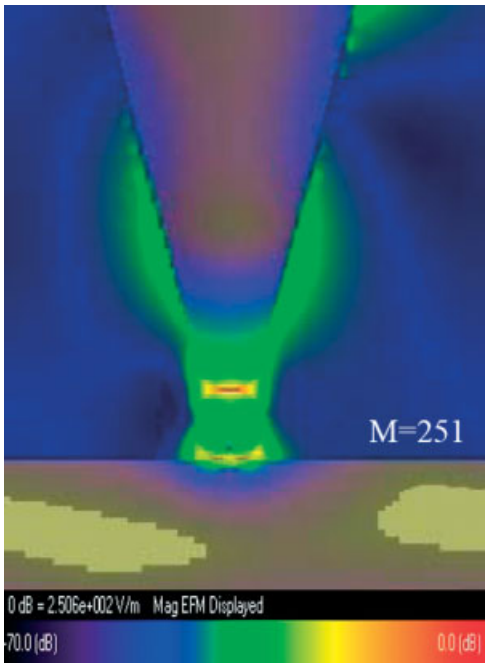

Figure 7. FDTD simulation of the electric field distribution in a double-tip TERS geometry. A 50-nm-diameter gold nanosphere was placed on the smooth gold surface. The tip parameters are as in Fig. 2(b). *M* is the maximum field enhancement.

Conclusions

In summary, we use a 3D-FDTD method to perform theoretical simulations of the field enhancement and spatial resolution of a gold conical tip, with and without a substrate, under side illumination. The TERS enhancement properties are found to be dependent on the tip size and shape, the substrate material, the tip–substrate distance, and the incidence angle and polarization of the excitation light. The dominating effect is the nano-gap effect between the metal tip and the metal substrate, where the strong plasmon coupling offers a tremendous TERS enhancement allowing even single-molecule detection. This TERS enhancement drops dramatically as the distance between the tip and the substrate increases. The spatial resolution of TERS is found to be mainly dependent on the radius of the curvature of the tip end and the distance between the tip and the substrate. A decrease of the tip radius can improve dramatically the spatial Raman resolution of TERS. Therefore, tips with sharp ends (small radius of curvature) should be preferable in TERS if high spatial resolution is required. Increasing the tip–substrate distance or changing the metallic substrate into a dielectric substrate will usually lower the spatial resolution.

Acknowledgments

H. Xu acknowledges the financial support from NSFC Grant No. 10625418, MOST Grant No. 2006DFB02020, 2007CB936800, and 'Bairen Project' of CAS. J. Aizpurua acknowledges financial support from the 'Intramural project' 200860I039 from CSIC and project FIS2007-66711-c01-01 from MEC. Z. Yang acknowledges financial support from NSFC Grant No. 20703032, MOST grant No. 2009CB930703 and the Natural Science Foundation of Fujian Province of China (No. E0710028).

References

[1] R. M. Stöckle, Y. D. Suh, V. Deckert, R. Zenobi, *Chem. Phys. Lett.* **2000**, *318*, 131.
[2] M. S. Anderson, *Appl. Phys. Lett.* **2000**, *76*, 3130.
[3] N. Hayazawa, Y. Inouye, Z. Sekkat, S. Kawata, *Opt. Commun.* **2000**, *183*, 333.
[4] B. Pettinger, B. Ren, G. Picardi, R. Schuster, G. Ertl, *Phys. Rev. Lett.* **2004**, *92*, 096101.
[5] B. Ren, G. Picardi, B. Pettinger, R. Schuster, G. Ertl, *Angew. Chem. Int. Ed.* **2005**, *44*, 139.
[6] M. A. Young, J. A. Dierger, R. P. Van Duyne, *Advances in Nano-Optics and Nano-Photonics* (Eds: S. Kavata, V. M. Shalaev), Elsevier: Amsterdam, **2007**, pp 1.
[7] Z. Q. Tian, B. Ren, J. F. Li, Z. L. Yang, *Chem. Commun.*, **2007**, *3514*, DOI: 10.1039/b616986d.
[8] H. Xu, J. Aizpurua, M. Kall, P. Apell, *Phys. Rev. E* **2000**, *62*, 4318.
[9] N. Anderson, P. Anger, A. Hartschuh, L. Novotny, *Nano Lett.* **2006**, *6*, 744.
[10] I. Notingher, A. Elfick, *J. Phys. Chem. B* **2005**, *109*, 15699.
[11] A. L. Demming, F. Festy, D. Richards, *J. Chem. Phys.* **2005**, *122*, 184716.
[12] R. M. Roth, N. C. Panoiu, M. M. Adams, R. M. Osgood Jr., C. C. Neacsu, M. B. Raschke, *Opt. Express* **2006**, *14*, 2921.
[13] J. N. Chen, W. S. Yang, K. Dick, K. Deppert, H. Q. Xu, L. Samuelson, H. X. Xu, *Appl. Phys. Lett* **2008**, *92*, 093110.
[14] W. Zhang, X. Cui, B. S. Yeo, T. Schmid, C. Hafner, R. Zenobi, *Nano Lett.* **2007**, *7*, 1401.
[15] J. P. Kottmann, O. J. F Martin, D. R. Smith, S. Schultz, *Chem. Phys. Lett.* **2001**, *341*, 1.
[16] M. Micic, N. Klymyshyn, Y. D. Suh, H. P. Lu, *J. Phys. Chem. B* **2003**, *107*, 1574.
[17] E. Hao, G. C. Schatz, *J. Chem. Phys.* **2004**, *120*, 357.
[18] L. D. Qin, S. L. Zou, C. Xue, A. Atkinson, G. C. Schatz, C. A. Mirkin, *Proc. Natl. Acad. Sci. U S A* **2006**, *103*, 13300.
[19] J. T. Krug II, E. J. Sanchez, X. S. Xie, *J. Chem. Phys.* **2002**, *116*, 10895.
[20] M. Futamata, Y. Maruyama, M. Ishikawa, *J. Phys. Chem. B* **2003**, *107*, 7607.
[21] C. Oubre, P. Nordlander, *J. Phys. Chem. B* **2005**, *109*, 10042.
[22] Z. Q. Tian, Z. L. Yang, B. Ren, J. F. Li, Y. Zhang, X. F. Lin, J. W. Hu, D. Y. Wu, *Faraday Discuss.* **2006**, *132*, 159.
[23] F. J. García de Abajo, J. Aizpurua, *Phys. Rev. B* **1997**, *56*, 15873.
[24] F. J. García de Abajo, A. Howie, *Phys. Rev. Lett.* **1998**, *80*, 5180.
[25] K. S. Yee, *IEEE Trans. Antennas Propag.* **1966**, *14*, 302.
[26] K. S. Kunz, R. J. Luebbers, *The Finite Difference Time Domain Method for Electromagnetics*, CRC Press, LLC: Boca Raton, **1993**.
[27] R. J. Luebbers, F. R. Hunsberge, K. S. Kunz, *IEEE Trans. Antennas Propag.* **1991**, *39*, 29.
[28] R. X. Bian, R. C. Dunn, X. S. Xie, P. T. Leung, *Phys. Rev. Lett.* **1995**, *75*, 4772.
[29] Z. Q. Tian, Z. L. Yang, B. Rene, D. Y. Wu, *Topics Appl. Phys.* **2006**, *103*, 125.
[30] M. Moskovits, L. L. Tay, J. Yang, T. Haslett, *Topics Appl. Phys.* **2002**, *82*, 215.
[31] H. Xu, E. J. Bjerneld, M. Kall, L. Borjesson, *Phys. Rev. Lett.* **1999**, *83*, 4357.
[32] J. Jiang, K. Bosnick, M. Maillard, L. Brus, *J. Phys. Chem. B* **2003**, *107*, 9964.
[33] P. P. Fang, J. F. Li, Z. L. Yang, L. M. Li, B. Ren, Z. Q. Tian, *J. Raman Spectrosc.* **2008**, *39*, 1679.
[34] O. J. F Martin, C. Girard, *Appl. Phys. Lett.* **1997**, *70*, 10.
[35] A. Cvitkovic, N. Ocelic, J. Aizpurua, R. Guckenberger, R. Hillenbrand, *Phys. Rev. Lett.* **2006**, *97*, 060801.